Expression of phenylalanine ammonia lyase as an intracellularly free and extracellularly cell surface-immobilized enzyme on a gut microbe as a live biotherapeutic for phenylketonuria

Yu Jiang[1†], Bingbing Sun[2,3†], Fenghui Qian[3], Feng Dong[3], Chongmao Xu[3], Wuling Zhong[4], Rui Huang[4], Qiwei Zhai[4], Yu Jiang[1*] & Sheng Yang[2*]

[1]*Shanghai Taoyusheng Biotechology Co., Ltd., Shanghai 201201, China;*
[2]*CAS Key Laboratory of Synthetic Biology, CAS Center for Excellence in Molecular Plant Sciences, Chinese Academy of Sciences, Shanghai 200032, China;*
[3]*Shanghai Research and Development Center of Industrial Biotechnology, Shanghai 201201, China;*
[4]*CAS Key Laboratory of Nutrition, Metabolism and Food Safety, Shanghai Institute of Nutrition and Health, Chinese Academy of Sciences, Shanghai 200031, China*

Phenylketonuria (PKU), a disease resulting in the disability to degrade phenylalanine (Phe) is an inborn error with a 1 in 10,000 morbidity rate on average around the world which leads to neurotoxicity. As an potential alternative to a protein-restricted diet, oral intake of engineered probiotics degrading Phe inside the body is a promising treatment, currently at clinical stage II (Isabella, et al., 2018). However, limited transmembrane transport of Phe is a bottleneck to further improvement of the probiotic's activity. Here, we achieved simultaneous degradation of Phe both intracellularly and extracellularly by expressing genes encoding the Phe-metabolizing enzyme phenylalanine ammonia lyase (PAL) as an intracellularly free and a cell surface-immobilized enzyme in *Escherichia coli* Nissle 1917 (EcN) which overcomes the transportation problem. The metabolic engineering strategy was also combined with strengthening of Phe transportation, transportation of PAL-catalyzed *trans*-cinnamic acid and fixation of released ammonia. Administration of our final synthetic strain TYS8500 with PAL both displayed on the cell surface and expressed inside the cell to the Pah^{F263S} PKU mouse model reduced blood Phe concentration by 44.4% compared to the control EcN, independent of dietary protein intake. TYS8500 shows great potential in future applications for PKU therapy.

phenylalanine ammonia lyase, cell surface display, phenylketonuria, TYS8500, oral administration

INTRODUCTION

The phenylalanine (Phe) metabolism pathway in a healthy body is mediated by phenylalanine hydroxylase (PAH, EC 1.14.16.1) and the requisite cofactor tetrahydrobiopterin (BH$_4$) to form tyrosine. Phenylketonuria (PKU) is an inborn error where a mutation causes a defect in PAH, resulting in an increase in Phe concentration and decrease in tyrosine concentration as well as presence of Phe metabolites (Smith et al., 2019). High levels of Phe is neurotoxic, causing irreversible and often severe intellectual impairment, autistic behavior, seizures, tremors, and ataxia (Bilder et al., 2017). PKU has been reported in all ethnic groups and its incidence

---

†Contributed equally to this work
*Corresponding authors (Sheng Yang, email: syang@sibs.ac.cn; Yu Jiang, email: yjiang@cibt.ac.cn)

varies widely around the world, affecting around one in every 10,000 births worldwide (van Spronsen, 2010). Newborn screening and diagnosis are initially undertaken in most countries in the first few weeks after birth and all cases are further screened for BH4 responsiveness. However, only about 30% of all PKU patients respond to BH_4 treatment by taking sapropterin dihydrochloride (KUVAN, BioMarin Pharmaceutical) (Al Hafid and Christodoulou, 2015). The prevailing and predominant treatment is restrictive dietary intake of Phe to a minimum that is required for normal growth, supplemented with specifically designed medical foods for patients including those that respond to BH_4 treatment. However, nutritional deficiencies as well as noncompliance due to poor palatability remains an issue. Furthermore, neurophysiological and neuropsychological impairments still persist in PKU patients even when treated with such therapy (Al Hafid and Christodoulou, 2015).

Gene therapies for expression of normal PAH in liver or muscle cells are at preclinical stages, but these treatments face challenges associated with the currently used gene transfer vectors, such as pre-existing neutralizing antibodies, potential immune responses, and the inability to transduce sufficient numbers of cells to be efficacious, indicating that this therapy may not be suitable for all patients and likely needs a substantial amount of time to develop (Isabella et al., 2018). PAH replacement therapy is not yet possible for PKU because of the instability of PAH as well as other related complexities (Levy et al., 2018). However, phenylalanine ammonia lyase (PAL, EC 4.3.1.24), a non-mammalian enzyme that converts Phe to *trans*-cinnamic acid (TCA) and ammonia holds promise as a non-dietary way to control Phe levels for patients with PKU. TCA has shown no embryotoxic effects in laboratory animals (Hoskins and Gray, 1982), and is excreted as hippurate in urine along with small amounts of cinnamate and benzoic acids (Hoskins et al., 1984). Pegvaliase (Palynziq, BioMarin Pharmaceutical), which was recently approved for treatment in adult patients, relies on systematic injection of a pegylated PAL (Markham, 2018); however, severe immune-mediated adverse reactions and anaphylaxis have been reported (Hydery and Coppenrath, 2019).

Oral administration of PAL is an alternative and rather safe therapy, thus suitable for PKU patients of all ages. In the early 1990s, researchers used orally administered encapsulated PAL extracted from yeast to control blood Phe levels in PKU patients (Hoskins et al., 1980) and Sprague-Dawley rats that were induced by chemical inhibition of PAH to be hyperphenylalanemic (Bourget and Chang, 1989), but the high cost associated with the production, stabilization and formulation of oral PAL at that time implied that it needed further development (Chang, 2005). A recombinant PAL mutant CDX-6114 reported to be resistant to low pH and protease degradation by enzyme evolution is currently at clinical stage I (NCT03577886), while its effectiveness when exposed within intestinal environment remains unknown.

The gut microbiome which naturally adapts to the intestinal environment offers an opportunity to regulate host metabolism either by production of nutrients or by degradation of dietary products that might otherwise be toxic (Chang, 2005). Researchers have reported a reduction of blood Phe levels in a mouse model of PKU ($Pah^{enu2/enu2}$) after oral administration of PAL-expressing *Escherichia coli* (Isabella et al., 2018; Sarkissian et al., 1999), *Lactococcus lactis* (Zhang et al., 2011), or *Lactobacillus reuteri* (Durrer et al., 2017), which suggests that microbial delivery of PAL as a therapy is promising for treating PKU. The only engineered strains that progressed to human clinical studies is SYNB1618 developed by Synlogic, which expressed PAL intracellularly in a probiotic *Escherichia coli* Nissle 1917 (EcN). EcN has been used to treat various gastrointestinal diseases and does not colonize humans (Isabella et al., 2018). However, the limited downregulation of blood Phe levels in PKU mice by SYNB1618 (Isabella et al., 2018) and the need to intake SYNB1618 at high level doses per day in its clinical study (Puurunen et al., 2021) indicate the necessity for further development of the engineered strain's activity (Puurunen et al., 2021).

Cell-surface display allows peptides and proteins to be displayed on the surface of microbial cells by fusing them with anchoring motifs. The protein to be displayed-the passenger protein-can be fused to an anchoring motif-the carrier protein-by N-terminal fusion, C-terminal fusion or sandwich fusion (Lee et al., 2003). Cell surface display of PAL offers a way to improve whole cell activity which is orthogonal to intracellularly expressed PAL. In addition, by being displayed on the cell surface, PAL can freely access intestinal Phe and membrane penetration of Phe will no longer be an issue. Here, we developed a biocatalyst to achieve simultaneous degradation of Phe both intracellularly and extracellularly in the intestinal tract (Lee et al., 2003).

RESULTS

Ice nucleation protein (INP)-fused PAL displayed on EcN surface can degrade Phe

The catalytic portion of the cell-surface displayed enzyme is located outside of the membrane, obviating the need for Phe transport into the cell. In this study, we assess three approaches for the surface display of a PAL from *Photorhabdus luminescens* in EcN. Constructs were made carrying *stlA* which codes for PAL that converts Phe to TCA, fused to the delivery portion of three different surface display systems: C-terminal of a poly-γ-glutamate synthetase complex PgsA from *Bacillus subtilis*, an unusual anionic polypeptide in which glutamate is polymerized via γ-amide linkages (Narita

et al., 2006), the C-terminal of the lipoprotein Lpp-OmpA chimera (Qu et al., 2015), and a truncated form of INP, InaK-N (N-terminal domain) from *Pseudomonas syringae* (Kang et al., 2008). The surface display system is controlled by *P*trc on the plasmid pTrcHis2B (Figure 1A). Results show that only INP-fused PAL could catalyze Phe to TCA (Figure 1B). One of the charged peptide, 6×Lys (K6), previously reported to increase the surface display efficiency (Liang et al., 2012) was added to each of the N-terminus of the three carrier proteins, and it was found that only the K6-InaK-N-fused PAL (K6INP-PAL) showed obvious activity toward Phe. Considering that inducible P*trc* was not suitable for future *in vivo* applications, it was replaced by a constitutive *P*j23119 which was reported to have a similar transcriptional activity with P*trc* (Cao et al., 2019), indicating that the significant increase in PAL activity was mainly the result of fused K6. The amount of TCA increased by 5.3 times compared to when K6 was not added (Figure 1B). To confirm whether the K6INP-PAL was successfully displayed on the cell surface, proteinase K was applied to digest the cell surface protein (Bradford, 1976; Liang et al., 2012; Zhang et al., 2016). The amount of TCA decreased by about 61% (Figure 1C), and the degradation of phenylalanine was reduced by 48.8% after a 3-h reaction compared to the cells without proteinase K applied (Figure 1D). We speculated that the surprising effects of K6 in promoting intracellular activity of PAL (Figure 1B) might be associated to protein folding and expression, such as fusion of a chaperone, while the exact mechanism remains to be investigated. These results demonstrated a successful application of the cell display strategy in the construction of Phe-degrading strains to realize extracellular Phe degradation for potential PKU therapy.

Metabolic engineering of EcN to degrade Phe intracellularly

In order to increase the whole cell Phe degradation activity, the intracellular and extracellular degradation module can be combined. To engineer EcN for intracellular Phe degradation, we integrated three copies of *stlA* controlled by a constitutive promoter *P*j23119, and two copies of *pheP*, a high-affinity Phe transporter that brings Phe into the cell (Isabella et al., 2018). We also integrated an arabinose-induced L-amino acid deaminase (LAAD), a membrane-associated enzyme that converts Phe to phenylpyruvate (PP) in the periplasm. LAAD requires oxygen for function, and is estimated to be functional in the microaerobic proximal small intestine (Isabella et al., 2018). When we continued to further increase the copy numbers of *stlA* controlled by the constitutive promoter *P*j23119, we found that the transformants grew very slowly, which was deemed to be caused by constitutive expression of *stlA*. Considering the potential metabolic stress from constitutive expression of PAL on cell

physiology including gene mutation on a large-scale and high cell density manufacturing processes that would be needed to produce clinical development batches, we then integrated two copies of isopropyl β-D-1-thiogalactopyranoside (IPTG)-inducible promoter *P*tac-controlled *stlA* to decouple cell growth and PAL expression to a certain extent, which generated TYS3308. These two copies of *stlA* increased the TCA production by 15.3% with a limited effect of its growth *in vitro* when induced by IPTG (Figure S1 in Supporting Information).

Phe was deaminated into TCA by PAL while releasing ammonia, which is estimated to diffuse into the intestine when the engineered strain was pharmaceutically applied. We speculated that the additional assimilation of ammonia into cell metabolites, such as amino acids, may accelerate PAL catalysis, especially under an environment with high ammonia concentration. Enhancement of L-arginine biosynthesis was targeted on the basis of the high nitrogen content of L-arginine (four atoms of nitrogen), and the strategy was applied in capturing gut ammonia in hyperammonemia models (Kurtz et al., 2019). We up-regulated arginine biosynthesis by deleting a negative regulator, *argR* of L-arginine biosynthesis, and mutated an L-arginine biosynthetic enzyme, *argA* into a feedback-resistant mutant *argA*Y19C (Figure 2A) (Kurtz et al., 2019). The resulting strain TYS8244 was found to produce 5.5% more TCA than that of its control TYS3308 (Figure 2B).

The addition of 2 mmol L^{-1} salicylic acid during the degradation of Phe by TYS8244 increased the concentration of extracellular TCA (Figure S2 in Supporting Information), indicating that salicylic acid induces TCA efflux, which was consistent with previous reports (Ravirala et al., 2007). The suspected salicylic acid-induced *acrA* or *emrA* transporter (Ravirala et al., 2007) was integrated into the *lacZ* site under the control of the constitutive promoter *P*j23119, and it was found that the *acrA*-expressing strain TYS8086 degraded Phe 1.2 times more than that of the original strain TYS8244, while TCA increased about 4% (Figure 2B). However, the strain expressing *emrA* did not affect TCA production (Figure S3 in Supporting Information).

We then optimized the ribosome binding site sequences of PheP and PAL by the Salislab online software (https://salislab.net/). The resulting strain TYS8499 increased TCA production by 6.9% compared with TYS8086 (Figure 2B). Expression of PAL in TYS8499 was also verified by SDS-PAGE as a specific band of ~57 kD (Figure S4 in Supporting Information).

Engineered EcN intracellularly and extracellularly degrades Phe

To further improve the ability of TYS8499 to degrade Phe, we added the cell surface display module to achieve si-
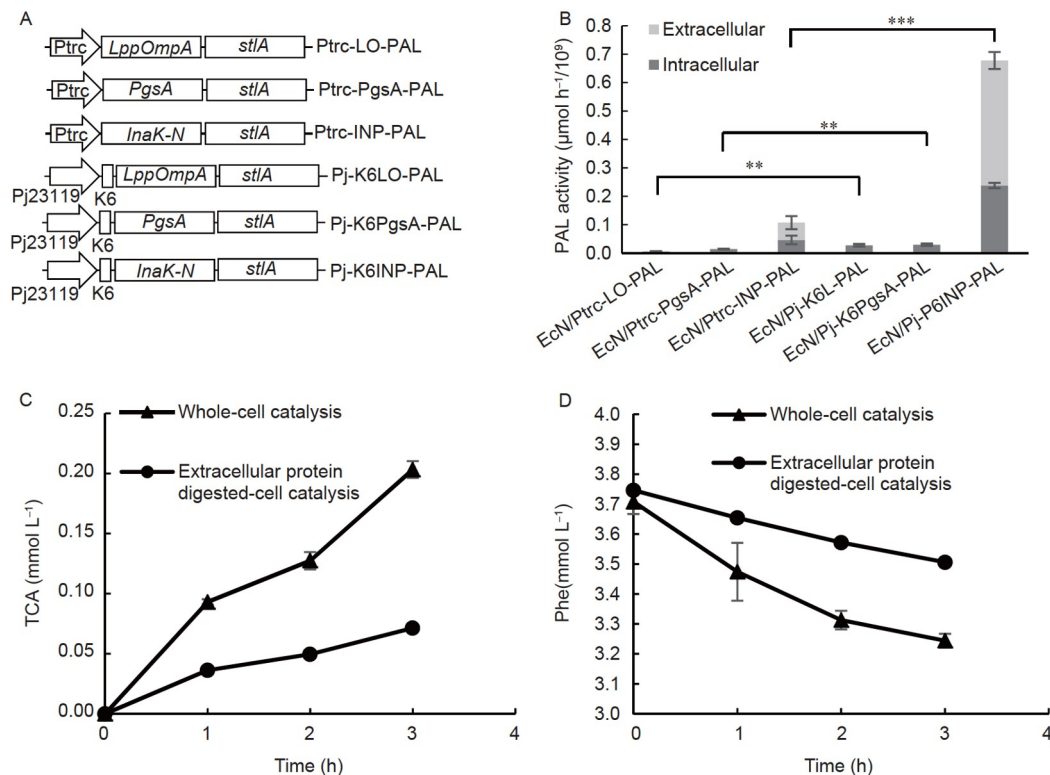
Figure 1 Recombinant EcN displaying PAL. A, pTtrcHis2B constructs carrying *stlA* coding for PAL, fused to the delivery portion of three different surface display systems: C-terminal of a poly-γ-glutamate synthetase complex PgsA from *Bacillus subtilis*, the C-terminal of the lipoprotein Lpp-OmpA chimera and a truncated form of the INP, InaK-N (N-terminal domain) from *Pseudomonas syringae*, with or without 6×Lys polypeptides (K6) anchored to the N-terminus of the carrier protein under an IPTG-inducible (*P*trc) or a constitutive promoter (*P*j23119); we analyzed $5×10^8$ activated cells in a 4 mmol L^{-1} Phe assay buffer for PAL activity. The intracellular activity was measured using cells under a proteinase K digestion in a 3 h reaction. B, The intracellular and extracellular activity of the 10^9 recombinant EcN carrying the six constructs indicated in (A). The rates of TCA synthesis (C) and Phe consumption (D) were calculated for recombinant EcN carrying plasmid Pj-K6INP-PAL. The extracellular activity was calculated as the whole cell activity minus the intracellular part. Bars represent the average±s.d. *, $P<0.05$; **, $P<0.01$; ***, $P<0.001$.

multaneous degradation of Phe intracellularly and extracellularly in the intestinal tract. Considering that the displayed PAL will be exposed to the intestinal environment, the ability to resist acid and protease degradation may help its activity (Figure 2A). Therefore, in addition to the PAL from *P. luminescens*, we also selected a PAL mutant from *Anabaena variabilis*, avPAL* (A39V, T54K, G59R, S73K, A91V, N290G, R305M, H307G, L407V, C503Q, Q521K, T524S, C565P), which is reported to be resistant to low pH and protease degradation by enzyme evolution (Huisman et al., 2014). We found that TYS8499 displaying K6-InaK-N fused avPAL* did not further increase the activity of TYS8499, while PAL from *P. luminescens* increased the production of TCA by 26.0% (Figure 2C). The K6-InaK-N fused PAL under control of *P*j23119 was then integrated into the *dapA* site of TYS8499, and the resulting strain TYS8516 produced 16.3% more TCA than TYS8499, indicating that the PAL activity in the surface display fraction determined by treating with Proteinase K in TYS8516 was about 16% of the whole cell activity (Figure 2D, E). The PAL activity of TYS8499 was not affected by Proteinase K (Figure S5 in Supporting Information). Deletion of the *dapA* gene, en-

coding 4-hydroxytetrahydropicolinate synthase, enables biocontainment that renders engineered bacteria dependent on exogenous diaminopimelate (DAP) for cell wall biosynthesis and growth (Isabella et al., 2018). The copy numbers of the surface display module integrated was then increased up to three to generate TYS8500 until the whole cell activity was equivalent to the K6-InaK-N fused PAL expression with plasmids (Figure S6A, B in Supporting Information).

The freezing viability effect on TYS8516 and TYS8500 that immobilized the surface displayed PAL was then investigated. It was found that the total and the extracellular activity did not change significantly within 4 weeks of cryopreservation, indicating its value for further pharmaceutical applications (Figure 2F, Figure S6C in Supporting Information).

In vivo activity of TYS8499, TYS8516 and TYS8500

In vivo activity and efficacy of TYS8499 (without PAL display), TYS8516 or TYS8500 (with PAL display) in *Pah*[F263S] mice are varied. *Pah*[F263S] is a common mutation in
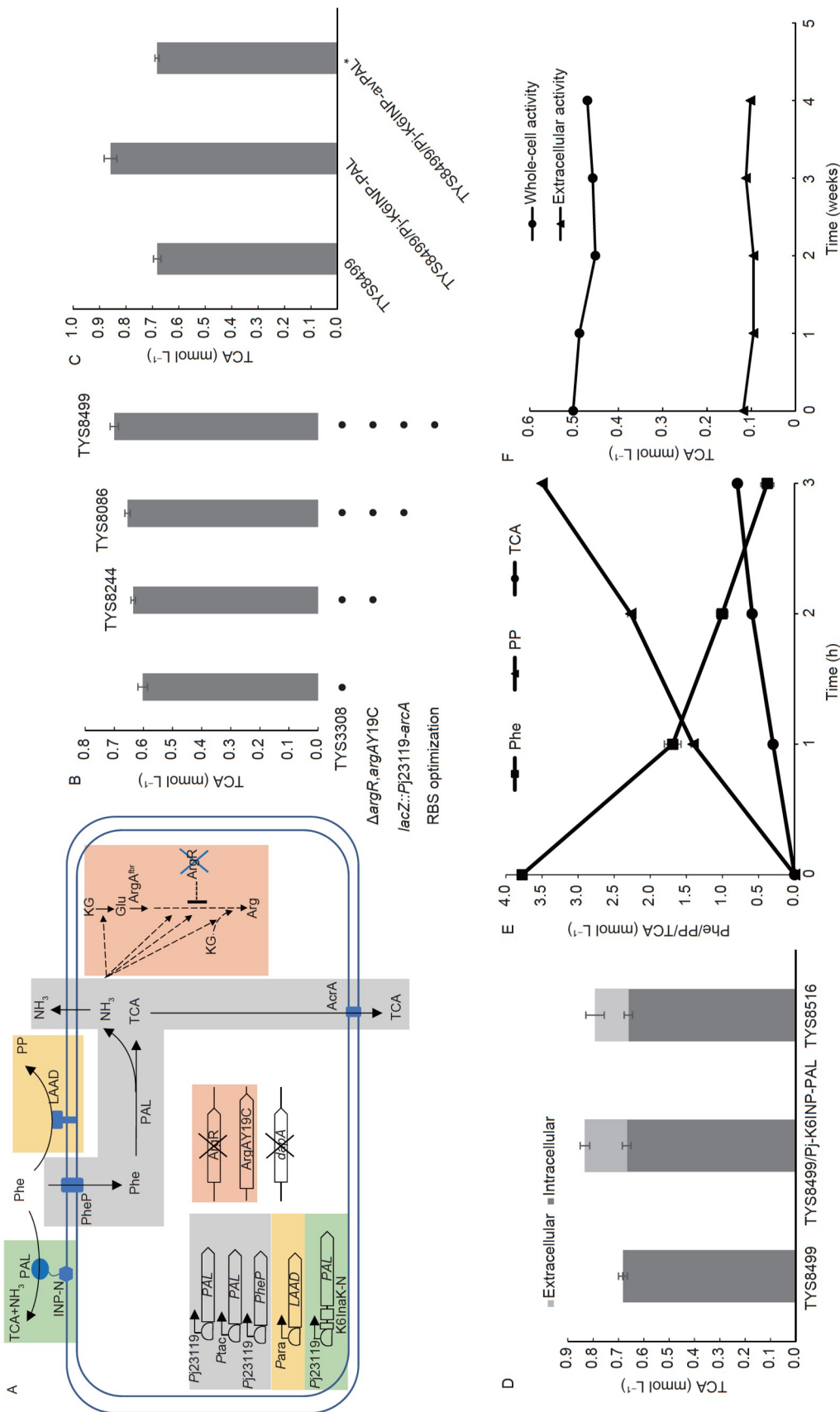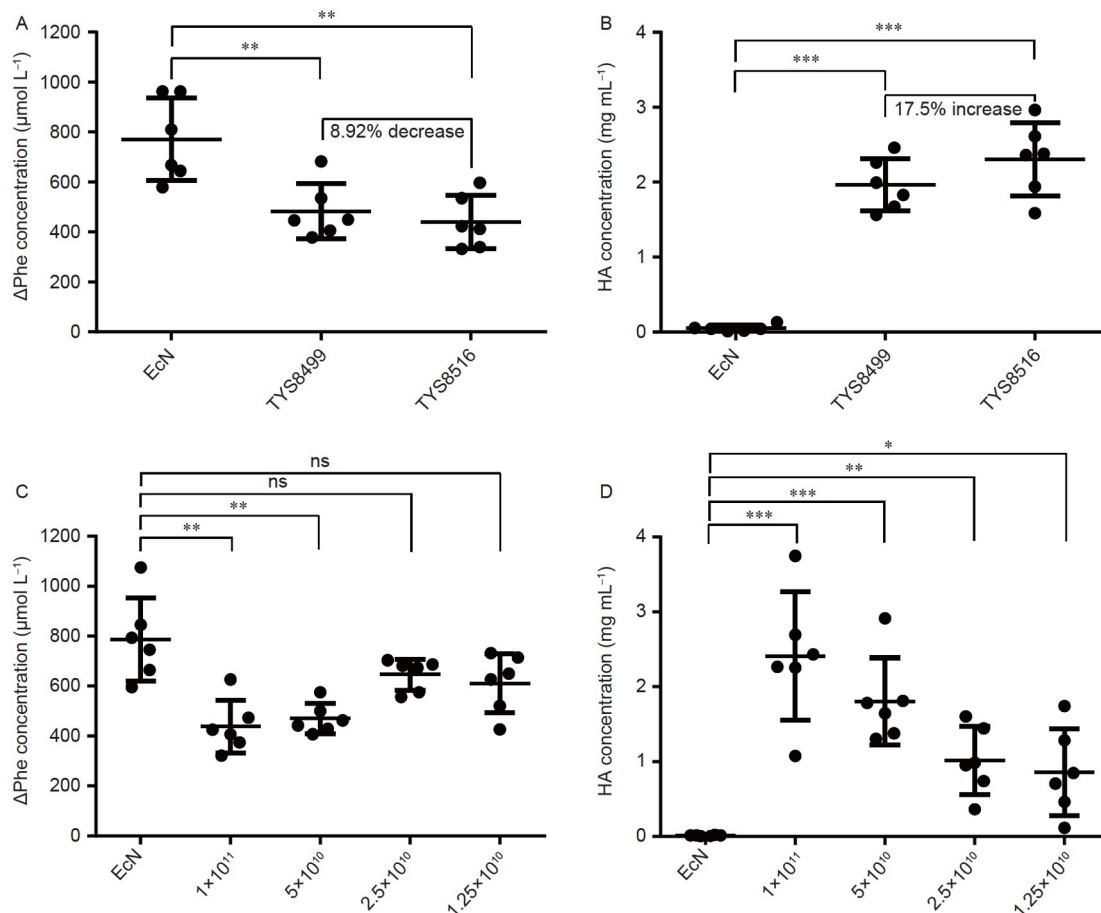
Figure 2 Engineering process and activity of a candidate therapeutic strain TYS8516 for PKU. A, TYS8516 contains chromosomally inserted genes for both intracellular and extracellular degradation of Phe. The gray shadowed pathway consists of PheP, a high-affinity Phe transporter that brings Phe into the cell, and PAL (*stlA*), which converts Phe into TCA, and AcrA, that encodes a predicated exporter. The orange shadowed pathway indicates enhanced L-arginine (Arg) synthesis in which an arginine repressor (*argR*) is deleted and feedback-resistant mutation Y19C in N-acetylglutamate synthase (*argA*) is applied. The yellow and green shadowed extracellar reaction consists of LAAD (*pma*), which converts Phe to PP with oxygen, and a displayed PAL fused to the N-terminal domain of INP. Regulation of these components is carried out by constitutive-, IPTG- and L-arabinose-inducible promoters to ensure their activities in the mammalian gut or *in vitro*. We analyzed 5×10^8 activated cells in 4 mmol L^{-1} Phe assay buffer for PAL activity. Intracellular Phe-degrading pathway optimized cells were engineered with (B) plasmids carrying an INP N-terminal domain-fused PAL from *P. luminescens* or a mutant (A39V, T54K, G59R, S73K, A91V, N290G, R305M, H307G, L407V, C503Q, Q521K, T524S, C565P) from *A. variabilis* (C), chromosomal integration of the INP N-terminal domain of TYS8516. D, (E) pre-induction using l-arabinose, IPTG. Levels of TCA, Phe or PP were calculated. The black bars display the average and s.d. of three independently prepared replicate samples. F, The long-term −70°C storage activity of TYS8516. *dapA*, codes for 4-hydroxytetrahydropicolinate synthase; K6, 6×Lys polypeptides; INP-N, a truncated form of the ice nucleation protein (INP), InaK-N (N-terminal domain) from P. syringae; KG, ketoglutarate; Glu, glutamate; TCA, *trans*-cinnamic acid; PP, phenylpyruvate; HA, hippuric acid. Bars represent the average±s.d.

PKU patients, and the genotype is consistent with $Pah^{enu2/enu2}$ mice which is widely used as the PKU animal model (Isabella et al., 2018). The coat color of the mutant mice was different from that of WT mice. The fur color gradually lightens with age and a fair-hair phenotype was observed, which was consistent with previous reports (Yin et al., 2022). It was previously reported that PP dosed orally in mice was not present in either blood or urine, suggesting it is not suitable for a biomarker. By contrast, over 90% of TCA is converted hepatically to hippuric acid (HA) and targeted for rapid urinary excretion in mice (Isabella et al., 2018). The serum Phe concentration in Pah^{F263S} mice is reduced to less than 200 μmol L^{-1} when maintained on a Phe-deficient diet. Although administration of activated TYS8516 did not ameliorate a significant increase in the levels of serum Phe than that of TYS8499 in Pah^{F263S} mice maintained on a Phe-deficient diet following subcutaneous (s.c.) Phe injection (38.0% *vs*. 34.0% decrease, Figure 3A), a significant increase in urinary HA excretion by TYS8516, 17.5% higher than that of TYS8499 was observed (Figure 3B). Subse-

quently, oral administration of activated TYS8516 in Pah^{F263S} mice resulted in dose-dependent serum Phe decrease and urinary HA recovery (Figure 3C, D). Further increase of PAL display integration module by TYS8500 showed a 9.84% increase in depletion of serum Phe and 9.44% increase in HA levels than that of TYS8516 with one copy of the PAL display module integrated (Figure S6D, E in Supporting Information).

DISCUSSION

Our engineered bacteria was constructed from the probiotic EcN, which has been safely used for nearly 100 years as an active pharmaceutical ingredient in multiple licensed medicinal products (Sonnenborn, 2016). In addition, free DAP levels were undetectable by liquid chromatography and mass spectrometry in the intestinal effluents of mice, and its concentration in soil was insufficient to support the growth of the engineered bacteria which contains a deletion of the

Figure 3 *In vivo* activity and efficacy of TYS8499 (without PAL display) and TYS8516 (with PAL display) in Pah^{F263S} mice. Pah^{F263S} mice on a Phe-deficient diet were housed and bled, followed by subcutaneous Phe administration (0.1 mg g^{-1} body weight) and an oral gavage of 5×10^{10} or an indicated dose of cells of EcN, TYS8499 or TYS8516 (A, C) ($n = 6$/group). The *y* axis represents the change in serum Phe before and 4 h after Phe injection. The horizontal line indicates the mean; error bars indicate s.d. (B), (D). Urine from the mice in (A), (C) was collected over 4 h and analyzed for HA. Bars represent the average±s.d. *, $P<0.05$; **, $P<0.01$; ***, $P<0.001$. ns: not significant.

dapA gene, thereby enabling *in vivo* and environmental biocontainment (Isabella et al., 2018). Using probiotics as a vector to express PAL is promising to realize daily intestinal intervention of PKU patients, which is clinically easier to manage than injection. The increased activity of PAL by intracellular expression in probiotic cells is limited by the transmembrane transport of Phe. By being displayed on the cell surface, PAL is free to access intestinal Phe and membrane penetration of the Phe is no longer an issue. In addition, cell surface display of PAL is orthogonal to intracellularly expressed PAL, which offers a way to improve the whole cell activity. Moreover, displaying PAL on cell surfaces of live probiotics have more advantages over free PAL, because live probiotics can continuously express and display PAL to resist degradation by proteases in the intestine, while the activity decrease of free PAL is irreversible after being degraded by proteases or deactivated by low pH. The whole cell activity of TYS8500 constructed in our study with three-copy of PAL integrated as the display module combined with intracellular PAL expression was 21.7% higher than TYS8499 that could only degrade Phe by intracellular PAL *in vitro*. Microbial cell-surface display has a wide range of biotechnological and industrial applications, including live vaccine development, peptide library screening, bioconversion using whole cell biocatalyst and bioadsorption (Lee et al., 2003). The first time of its expanded application in engineering gut microbiome offers a new way to regulating human metabolism.

We noticed that the decrease of serum Phe is not that consistent with the increase in HA in urine in TYS8516 with PAL displayed compared with TYS8499 without PAL displayed. We assumed that the decrease of serum Phe to a certain extent is buffered by *in vivo* circulation and does not appear to be significant. Although microbial cell-surface display is a rather well-established technology, the characteristics of carrier proteins, passenger proteins, host cell, and fusion methods all affect the efficiency of surface display (Lee et al., 2003). Three display systems were tested for PAL in our study, and further optimization showed about half of the PALs was successfully displayed. The significant display efficiency improvement by the addition of polypeptide K6 to InaK-N might be associated with the N-terminal pI-specific directionality and their interactions with InaK-N, but the molecular mechanism of how the charged polypeptides affect the surface display of INP remains unclear (Zhang et al., 2016). We do not think that further improving display efficiency is the most important aspect of future strain optimization, because we have seen that by increasing the copy number of PAL display modules, whole cell vitality has reached its limit. We speculate that this is due to space constraints on the cell surface. According to the recently announced SYNB1618 clinical phase II results, PKU patients experienced a 20%–40% reduction in D5-Phe after

meals. The TYS8500 constructed in this article showed 16.8% more degradation of Phe activity *in vivo* than SYNB1618 according to their published data (Isabella et al., 2018), which has potential in future treatment of PKU. We also believe that the strain needs to be further optimized to increase its activity, because the 20%–40% reduction of Phe is not enough to satisfy clinical needs. We believe that the future direction for optimization is to select PALs with higher activity (Adolfsen et al., 2021). This can be achieved through natural selection (Hyun et al., 2011) or protein engineering. The latter requires the establishment of high-throughput screening methods (Mays et al., 2020).

MATERIALS AND METHODS

All strains and plasmids constructed in this study are listed in Table S1 in Supporting Information. The primers used for plasmid construction and genetic modifications are listed in Table S2 in Supporting Information.

Construction of plasmids for cell surface display

For the construction of plasmids Ptrc-PgsA-PAL, Ptrc-LO-PAL and Ptrc-INP-PAL, the *pgsA* gene was PCR-amplified from *B. subtilis* using primers pgsA(trc)-F/pgsA(trc)-R; the *lpp-ompA* gene was amplified from *E. coli* using primers lpp(trc)-F/lpp(trc)-R and ompA(trc)-F/ompA(trc)-R; the inaK-N gene was amplified from pUC-inaK synthesized by GenScript (Nanjing, China); the PAL gene was amplified by PCR from pUC-stlA synthesized by GenScript. All of the DNA fragments were cloned into the *Nco*I/*Hind*III lincarized pTrcHis2B vector using a DNA assembly Kit (TransGen Biotech) to generate Ptrc-PgsA-PAL, Ptrc-LO-PAL and Ptrc-INP-PAL.

Plasmids Pj-K6INP-PAL bears 6×Lys added to the 5′ end of inaK-N, inaK-N and PAL from Ptrc-INP-PAL controlled by the *P*j23119 promoter. The p15A replicon fragment was amplified from the pSU2718 vector using 15A-F/Psu-RG primers, and the kanamycin resistance gene was PCR-amplified from the pPIC9k vector using Kan-FG/Kan-R(15A) primers. The inaK-N gene in Pj-K6INP-PAL was replaced with *pgsA* or *lpp-ompA* to generate Pj-K6PgsA-PAL or Pj-K6LO-PAL. The PAL gene in Pj-K6INP-PAL was replaced with avPAL* synthesized by GenScript to generate Pj-K6INP-avPAL*.

Construction of Phe-degrading strains

Different plasmids for cell surface display were transformed into the EcN by electroporation to generate recombinant Nissle 1917 strains displaying PAL.

Phe-degrading strains also had genes inserted into the EcN

chromosome using CRISPR/Cas methods (Li et al., 2021). Three copies of PAL controlled by the Pj23119 promoter were integrated into *malE/K*, *yicS/nepI* and *malP/T* sites. Two copies of PAL controlled by the tac promoter were inserted into *exo*/cea and *rhtC/B* integration sites. Three copies of surface displaying PAL genes fused with inaK-N for its concurrent expression controlled by the Pj23119 promoter were integrated into *dapA*, *betA* and *ybaP* sites, which did not affect the growth (Goormans et al., 2020; Isabella et al., 2018; Li et al., 2021). Two copies of PheP which expressed the Phe transporter from *E. coli* controlled by Pj23119 were inserted into *lacZ* and *agaI* sites. One copy of Pma which encoded a L-amino acid deaminase from *P. mirabilis* controlled by the P_{BAD} promoter was integrated into the *araBC* site. The efflux pump gene *acrA* or *emrA* was overexpressed by the Pj23119 promoter. ArgR deletion and ArgAY19C mutation for a feedback-resistant version were done also using CRISPR/Cas methods.

The ribosome-binding sites (RBSs) of PAL and PheP controlled by Pj23119 were optimized using webinterface RBSonline calculator (https://salislab.net/) to achieve a targeted translation initiation rate. The optimized RBSs sequences were listed in Table S3 in Supporting Information.

PAL activity assay *in vitro*

The recombinant strains were cultured in tubes containing 4 mL LB medium, and cultivated overnight at 37 °C, 250 r min^{-1}. 1% of the overnight culture was transferred to a shake flask containing 30 mL LB medium, and incubated for 1.5 h at 37 °C, 250 r min^{-1}. Then 1 mmol L^{-1} IPTG was added and the incubation continued for 3 h.

The cells were collected by centrifugation at 4,000 r min^{-1}, resuspended in M9 medium (containing 0.5% glucose), and the OD$_{600}$ was adjusted to 1.0. 0.4 mL of the supernatants were removed into 5 mL of activity assay buffer (M9 medium, 5 g L^{-1} glucose, 50 mmol L^{-1} MOPS, 4 mmol L^{-1} L-phenylalanine, and with or without 2 mmol L^{-1} salicylate), and incubated at 250 r min^{-1} at 37°C for 3 h with shaking. The sample was collected, centrifuged at 13,000 r min^{-1} for 10 min, and the supernatant was detected by high performance liquid chromatography (HPLC).

Assay for outer membrane's fraction of surface displaying PAL

The recombinant strains were centrifuged and washed with a phosphate-buffered saline (PBS) buffer, then adjusted to an OD$_{600}$ value of 1.0. Samples were treated with Proteinase K (0.1 mg mL^{-1}) at 37°C. After 1 h of incubation, cells treated and untreated with Proteinase K were assayed for PAL activity as described above (Liang et al., 2012).

SDS-PAGE Analysis

An equal volume (10 µL, ~0.1 OD) of each fraction was mixed with the loading buffer, boiled for 10 min, and resolved by 10% (wt/vol) SDS-polyacrylamide gel electrophoresis (SDS-PAGE).

Recombinant strain culturing in a bioreactor

Cultures were placed in a 2-liter bioreactor (New Brunswick Scientific, NBS) with a working volume of 1 L. A single colony was picked and inoculated in a tube containing 4 mL LB (containing 0.1 g L^{-1} DAP, purchased from Sigma), and cultivated overnight at 37°C, 220 r min^{-1}. The overnight culture broth was transferred to a 500 mL shake flask containing 100 mL of fermentation medium (Y.E 24 g L^{-1}, Soy peptone 12 g L^{-1}, K$_2$HPO$_4$ 11.4 g L^{-1}, KH$_2$PO$_4$ 1.7 g L^{-1}, Glycerol 32 mL L^{-1}, DAP 0.3 g L^{-1}) at 1% inoculum, and cultured for 8 h.

The shake flask culture was transferred to a 2 L NBS self-controlled fermentor containing 1 L fermentation medium at a 1% inoculum. The temperature was controlled at 37°C, and the dissolved oxygen was controlled at 60%. When OD$_{600}$ reached 1.5, 1 mmol L^{-1} IPTG was added and the dissolved oxygen was controlled at above 30%. After 12 h of continuous cultivation, the final concentration of 0.15% L-arabinose was added for 1 h induction. During the whole fermentation process, the pH was controlled at 7.0 with ammonia water. The cells were collected by centrifugation at 4,500×*g* for 30 min at 4°C, resuspended in a PBS solution containing 15% sterile glycerol, and stored at −80°C.

The recombinant strain activity and efficacy *in vivo*

Pah^{F263S} mice (purchased from GemPharmatech Co. Nanjing, China) were fed with Phe-deficient diet (purchased from Deyts), and drinking water containing phenylalanine (0.5 g L^{-1}) was used to supplement Phe-deficient diet. At the beginning of the study (*T*=0 h), the phenylalanine-containing drinking water supply was replaced with regular drinking water, and blood was collected to detect serum phenylalanine at *T*=0 h. Then the mice were injected subcutaneously with Phe (0.1 mg g^{-1}, BW). 300 µL of the recombinant strains or EcN were orally gavaged at 1, 2, and 3 h post injection. Blood and urine were collected 4 h post injection for serum Phe and hippuric acid assay.

Dose response assay *in vivo*

The difference between this assay and the one above was the total number of gavage viable bacteria. For dose response and efficacy determination, oral gavage was 1×10^{11} cfu, 5×10^{10} cfu, 2.5×10^{10} cfu or 1.25×10^{10} cfu. Blood and urine

collection were carried out as described above.

Determination of L-phenylalanine, phenylpyruvate and *trans*-cinnamic acid levels by HPLC

Determination of L-phenylalanine, phenylpyruvate and *trans*-cinnamic acid levels *in vitro* were done using HPLC. The HPLC system consisted of the Chromatographic column ZORBAX SB-C18 (150 mm×4.6 mm, 5 μm) and the UV detector. The injection volume used was 5 μL. 1.5% acetic acid and acetonitrile were used as mobile phases for gradient elution, 1.5% CH_3COOH/CH_3CN (95/5) was used from 0 to 8 min, and 1.5% CH_3COOH/CH_3CN (0/100) was used from 13.1 to 23 min. The detection wavelength was 260 nm and the column temperature was 40°C.

The assay of serum phenylalanine

2 μL of serum was suspended with 198 μL of pre-cooled 80% methanol for 1 min, then placed in an ice bath and sonicate for 30 min, incubated at −20°C for 2 h and centrifuged at 13,000×*g* for 15 min at 4°C. 40 μL of supernatant was transferred to a new 1.5 mL centrifuge tube and freeze-dried overnight. 400 μL of 0.1% formic acid was added to resuspend, and the solution was sonicated for 30 min in an ice bath again.

Mobile phase A was 0.1% formic acid and mobile phase B was 0.1% fromic acid in methanol. Chromatographic separation was carried out with the following gradient: 2% B from 0 to 5 min, 2%→40% B from 5 to 6 min, 40%→90% B from 6 to 7.5 min, 90%→2% B from 7.5 to 8 min, and the flow rate was 200 μL min^{-1}. Multipe reaction monitoring in positive 5500 V mode was used for trandem MS analysis. The compound-depnedent LC-MS/MS parameters were: Q1 mass: 166.2, Q3 mass: 120.2, curtain gas (CUR): 10 psi, declustering potential (DP): 125 V, collision energy (CE): 16 V, and cell exit potential (CXP): 13 psi.

Determination of HA levels in urine by HPLC

100 μL methanol was added to 100 μL of urine specimens and centrifuged at 2,500 r min^{-1} for 5 min. Finally, 3 μL of the supernatant was injected into HPLC. The HPLC mobile phase consisted of a mixture of 5 mmol L^{-1} KH_2PO_4 (pH 2.5)/CH_3CN (90/10). The column used was SB-C18 (4.6 mm×150 mm, Agilent, USA). The effluent was monitored at 225 nm and the total assay was carried out at 25°C (Duydu et al., 1999). Hippuric acid was purchased from Sigma.

References

Adolfsen, K.J., Callihan, I., Monahan, C.E., Greisen Per, J., Spoonamore, J., Momin, M., Fitch, L.E., Castillo, M.J., Weng, L., Renaud, L., et al. (2021). Improvement of a synthetic live bacterial therapeutic for phenylketonuria with biosensor-enabled enzyme engineering. Nat Commun 12, 1–3.

Al Hafid, N., and Christodoulou, J. (2015). Phenylketonuria: a review of current and future treatments. Transl Pediatrics, 4, 304–317.

Bilder, D.A., Kobori, J.A., Cohen-Pfeffer, J.L., Johnson, E.M., Jurecki, E. R., and Grant, M.L. (2017). Neuropsychiatric comorbidities in adults with phenylketonuria: a retrospective cohort study. Mol Genet Metab 121, 1–8.

Bourget, L., and Chang, T.M.S. (1989). Effects of oral administration of artificial cells immobilized phenylalanine ammonia-lyase on intestinal amino acids of phenylketonuric rats. Biomater Artif Cells Artif Organs 17, 161–181.

Bradford, M.M. (1976). A rapid and sensitive method for the quantitation of microgram quantities of protein utilizing the principle of protein-dye binding. Anal Biochem 72, 248–254.

Cao, Y., Song, M., Li, F., Li, C., Lin, X., Chen, Y., Chen, Y., Xu, J., Ding, Q., and Song, H. (2019). A synthetic plasmid toolkit for *Shewanella oneidensis* MR-1. Front Microbiol 10, 410.

Chang, T.M.S. (2005). Therapeutic applications of polymeric artificial cells. Nat Rev Drug Discov 4, 221–235.

Durrer, K.E., Allen, M.S., and Hunt von Herbing, I. (2017). Genetically engineered probiotic for the treatment of phenylketonuria (PKU); assessment of a novel treatment *in vitro* and in the PAHenu2 mouse model of PKU. PLoS ONE 12, e0176286.

Duydu, Y., SÜZen, S., Vural, N., Erdem, N., Uysal, H. (1999). A modified method for determination of hippuric acid in urine by HPLC. Ankara Universitesi Eczacilik Fakultesi Dergisi, 28, 37–46.

Goormans, A.R., Snoeck, N., Decadt, H., Vermeulen, K., Peters, G., Coussement, P., Van Herpe, D., Beauprez, J.J., De Maeseneire, S.L., and Soetaert, W.K. (2020). Comprehensive study on *Escherichia coli* genomic expression: does position really matter? Metab Eng 62, 10–19.

Hoskins, J.A., and Gray, J. (1982). Phenylalanine ammonia lyase in the management of phenylketonuria: the relationship between ingested cinnamate and urinary hippurate in humans. Res Commun Chem Pathol Pharmacol, 35, 275–282.

Hoskins, J.A., Holliday, S.B., and Greenway, A.M. (1984). The metabolism of cinnamic acid by healthy and phenylketonuric adults: a kinetic study. Biol Mass Spectrom 11, 296–300.

Hoskins, J.A., Jack, G., Peiris, R.J.D., Starr, D.J.T., Wade, H.E., Wright, E. C., and Stern, J. (1980). Enzymatic control of phenylalanine intake in phenylketonuria. Lancet 315, 392–394.

Huisman, G.W., Agard, N.J., Mijts, B., Vroom, J., Zhang, X., Huisman, G., and Agard, N. (2014). New engineered polypeptide useful in pharma-

ceutical composition for treating phenylketonuria, has phenylalanine ammonia-lyase (PAL) activity, comprises specific amino acid sequence. US Patent, 2014314843-A1.

Hydery, T., and Coppenrath, V.A. (2019). A comprehensive review of pegvaliase, an enzyme substitution therapy for the treatment of phenylketonuria. Drug Target Insights 13.

Hyun, M.W., Yun, Y.H., Kim, J.Y., and Kim, S.H. (2011). Fungal and plant phenylalanine ammonia-lyase. Mycobiology 39, 257–265.

Isabella, V.M., Ha, B.N., Castillo, M.J., Lubkowicz, D.J., Rowe, S.E., Millet, Y.A., Anderson, C.L., Li, N., Fisher, A.B., West, K.A., et al. (2018). Development of a synthetic live bacterial therapeutic for the human metabolic disease phenylketonuria. Nat Biotechnol 36, 857–864.

Kang, D.G., Li, L., Ha, J.H., Choi, S.S., and Cha, H.J. (2008). Efficient cell surface display of organophosphorous hydrolase using N-terminal domain of ice nucleation protein in *Escherichia coli*. Korean J Chem Eng 25, 804–807.

Kurtz, C.B., Millet, Y.A., Puurunen, M.K., Perreault, M., Charbonneau, M. R., Isabella, V.M., Kotula, J.W., Antipov, E., Dagon, Y., Denney, W.S., et al. (2019). An engineered *E. coli* Nissle improves hyperammonemia and survival in mice and shows dose-dependent exposure in healthy humans. Sci Transl Med 11, eaau797.

Lee, S.Y., Choi, J.H., and Xu, Z. (2003). Microbial cell-surface display. Trends Biotechnol 21, 45–52.

Levy, H.L., Sarkissian, C.N., and Scriver, C.R. (2018). Phenylalanine ammonia lyase (PAL): from discovery to enzyme substitution therapy for phenylketonuria. Mol Genet Metab 124, 223–229.

Li, Q., Sun, B., Chen, J., Zhang, Y., Jiang, Y., and Yang, S. (2021). A modified pCas/pTargetF system for CRISPR-Cas9-assisted genome editing in *Escherichia coli*. Acta Biochim Biophys Sin 53, 620–627.

Liang, B., Li, L., Mascin, M., and Liu, A. (2012). Construction of xylose dehydrogenase displayed on the surface of bacteria using ice nucleation protein for sensitive D-xylose detection. Anal Chem 84, 275–282.

Markham, A. (2018). Pegvaliase: first global approval. BioDrugs 32, 391–395.

Mays, Z.J., Mohan, K., Trivedi, V.D., Chappell, T.C., and Nair, N.U. (2020). Directed evolution of *Anabaena variabilis* phenylalanine ammonia-lyase (PAL) identifies mutants with enhanced activities. Chem Commun 56, 5255–5258.

Narita, J., Okano, K., Tateno, T., Tanino, T., Sewaki, T., Sung, M.H., Fukuda, H., and Kondo, A. (2006). Display of active enzymes on the cell surface of *Escherichia coli* using PgsA anchor protein and their application to bioconversion. Appl Microbiol Biotechnol 70, 564–572.

Puurunen, M.K., Vockley, J., Searle, S.L., Sacharow, S.J., Phillips Iii, J.A., Denney, W.S., Goodlett, B.D., Wagner, D.A., Blankstein, L., Castillo, M.J., et al. (2021). Safety and pharmacodynamics of an engineered *E. coli* Nissle for the treatment of phenylketonuria: a first-in-human phase 1/2a study. Nat Metab 3, 1125–1132.

Qu, W., Xue, Y., and Ding, Q. (2015). Display of fungi xylanase on *Escherichia coli* cell surface and use of the enzyme in xylan biodegradation. Curr Microbiol 70, 779–785.

Ravirala, R.S., Barabote, R.D., Wheeler, D.M., Reverchon, S., Tatum, O., Malouf, J., Liu, H., Pritchard, L., Hedley, P.E., Birch, P.R.J., et al. (2007). Efflux pump gene expression in *Erwinia chrysanthemi* is induced by exposure to phenolic acids. Mol Plant Microbe Interact 20, 313–320.

Sarkissian, C.N., Shao, Z., Blain, F., Peevers, R., Su, H., Heft, R., Chang, T. M.S., and Scriver, C.R. (1999). A different approach to treatment of phenylketonuria: phenylalanine degradation with recombinant phenylalanine ammonia lyase. Proc Natl Acad Sci USA 96, 2339–2344.

Smith, N., Longo, N., Levert, K., Hyland, K., and Blau, N. (2019). Phase I clinical evaluation of CNSA-001 (sepiapterin), a novel pharmacological treatment for phenylketonuria and tetrahydrobiopterin deficiencies, in healthy volunteers. Mol Genet Metab 126, 406–412.

Sonnenborn, U. (2016). *Escherichia coli* strain Nissle 1917—from bench to bedside and back: history of a special *Escherichia coli* strain with probiotic properties. FEMS Microbiol Lett 363, fnw212.

Yin, S., Ma, L., Shao, T., Zhang, M., Guan, Y., Wang, L., Hu, Y., Chen, X., Han, H., Shen, N., et al. (2022). Enhanced genome editing to ameliorate a genetic metabolic liver disease through co-delivery of adeno-associated virus receptor. Sci China Life Sci 65, 718–730.

van Spronsen, F.J. (2010). Phenylketonuria: a 21st century perspective. Nat Rev Endocrinol 6, 509–514.

Zhang, Y., Jia, X., Wang, L., Liu, J., and Ma, G. (2011). Preparation of Ca-Alginate microparticles and its application for phenylketonuria oral therapy. Ind Eng Chem Res 50, 4106–4112.

Zhang, Z., Tang, R., Bian, L., Mei, M., Li, C., Ma, X., Yi, L., and Ma, L. (2016). Surface immobilization of human arginase-1 with an engineered ice nucleation protein display system in *E. coli*. PLoS ONE 11, e0160367.

SUPPORTING INFORMATION

The supporting information is available online at https://doi.org/10.1007/s11427-021-2137-3. The supporting materials are published as submitted, without typesetting or editing. The responsibility for scientific accuracy and content remains entirely with the authors.